Volume 14, Issue 1, 142301 (1-9)

International Journal Industrial Chemistry (IJIC)

https://dx.doi.org/10.57647/j.ijic.2023.1401.01

Nitrate ion removal with new nanocomposite based on vermiculite

Ehsan Ghorbannezhad[1], Susan Khosroyar[1]*, Farzad Kaj[2]

[1]*Department of Chemical Engineering, Quchan Branch, Islamic Azad University, Quchan, Iran.*
[2]*Department of Agriculture and Environmental Engineering, Rostock University, Rostock, Deutschland.*

***Corresponding author**: susankhosroyar@yahoo.com

Original Research

Received:
17 October 2022
Revised:
28 November 2022
Accepted:
30 December 2022
Published online:
30 March 2023

Abstract:

The vermiculite/aluminum oxide nanocomposite absorbent was investigated in this study using the gel decomposition method under the influence of ultrasound waves. It placed. It can absorb nitrate ions. Different analyses identified the adsorbents; the initial concentration, temperature, amount of adsorbent, contact time, and pH were evaluated in this case. Other isotherm models were used in the adsorption mechanism and control steps. The results show that Langmuir isotherm and second-order kinetics have the best match. Based on the results, it was revealed that the above adsorbent is suitable for aqueous solutions.

Keywords: Kinetics; Nitrate; Adsorption isotherm; Vermiculite; Aluminum oxide

1. Introduction

Water plays a crucial role in human development and life events. However, human development has increased water consumption and pollution, a society's primary concern. The presence of low levels of toxic mineral anions in water is a severe threat to human health [1]. Among these anions, Nitrate is one of the most essential elements worldwide and is considered a water pollutant [2]. Nitrate is a colorless, odorless, and tasteless ion that is highly soluble in water and not easily detectable in drinking water without testing. It is found in water at concentrations below the permissible limit. Nitrate ions are not toxic, but their reduction to nitrite by microorganisms can pose serious health risks, especially for infants under six months. Since the stomach acid of infants is not as strong as that of adults, it leads to the formation of bacteria that convert nitrates into nitrites [3]. The absorbed nitrites in the blood can convert hemoglobin into methemoglobin, which is particularly dangerous for infants. Nitrate ions can also have long-term effects, including the formation of cancerous tumors in the liver, kidneys, stomach, mouth, nasal cavity, lungs, esophagus, and diabetes [4].

Furthermore, aquatic organisms, especially freshwater ecosystems, are most affected by excessive nitrates in water and the resulting toxicity. Excessive nitrogen in surface waters increases the growth of algae and is known as eutrophication, the leading cause of oxygen depletion in lakes and rivers [4]. Algal growth in water has direct and indirect consequences for human health. The absorption of neurotoxins in algae by certain fish and the closure of the water's respiratory surface in effluents for plants are among the consequences of algal growth [5]. Removing nitrates from environmental sources such as surface and groundwater is one of the prerequisites for preventing such consequences [6].

Standard technologies for nitrate removal include ion exchange, adsorption, chemical reduction, reverse osmosis, and electrodialysis. Reverse osmosis and electrodialysis are methods used in recent years to reduce nitrogen in water [5]. One of the advantages of these methods is the possibility of automating their operation. Also, these systems do not need precise control of operational conditions. However, these technologies are limited for nitrate removal due to the high cost of equipment, high energy consumption, and high sludge production. Surface adsorption is a standard process to reduce nitrate levels in water [7].

Compounds used in surface adsorption include nanocomposites. In recent years, surface adsorption by nanocomposites has been used to remove pollutants and harmful ions [8].

Nanocomposites are compounds that contain nano-scale components to form nano-scale particles that efficiently adsorb surface pollutants and thus have a large specific surface area [9]. Vermiculite-based nanocomposites can be mentioned as compounds used in surface adsorption. Vermiculite is composed of expandable minerals [10]. The presence of metal oxide nanoparticles, such as aluminum oxide, can give unique properties to nanocomposites [11]. In the present study, a nanocomposite of vermiculite-aluminum oxide was used to prepare the nanocomposite. The sol-gel degradation method was used to prepare this nanocomposite under ultrasonic waves. Subsequently, the prepared nanocomposite was characterized, and its performance in an aqueous environment containing nitrate ions was investigated.

2. Experimental section

2.1 Materials

Sadra Chemistry Company prepared Vermiculite to produce nanocomposites. Zinc acetate, citric acid, and hydrochloric acid were purchased from Sigma Aldrich. Potassium nitrate for preparing stock solution was obtained from Kian Kaveh Azma Company.

2.2 Methods

2.2.1 Synthesis of nanocomposites

To synthesize nanocomposites, it is initially necessary to activate vermiculite. For chemical activation of vermiculite, 10 grams of raw vermiculite are mixed with 50 mL of 1 Molar hydrochloric acid in a magnetic stirrer for one day. Then, this homogeneous mixture is transferred to the ultrasonic bath for 4 hours, and the resulting suspension is centrifuged and washed several times with DI water. The resulting vermiculite is placed in an oven at 100 ^{o}C (for 12 hours). This experiment is repeated using 2 Molar hydrochloric acid. The sol-gel method is used to prepare vermiculite/aluminum oxide nanocomposites. First, activated vermiculite is added to the vessel during the production of aluminum oxide nanoparticles. To determine the weight percentages of different nanocomposites, the weight of aluminum oxide nanoparticles is chosen as the basis, and the amount of vermiculite will vary depending on the sample percentage. For this reason, zinc acetate and citric acid are dissolved in distilled water and stirred together for 1 hour. This solution is considered as solution number one.

Next, starch is dissolved in distilled water and heated to 60 ^{o}C (solution number two). Solution number one is added to solution number two and stirred together for half an hour. A certain amount of activated vermiculite is added to the above mixture and then transferred to an ultrasonic bath for 2 hours at 60 ^{o}C. The resulting gel is placed in an oven at 60^{o}C for 12 hours until dried. Finally, the sample is placed in a furnace at 350 ^{o}C for 2 hours to burn off organic materials and then in a furnace at 600 ^{o}C for 2 hours for calcination. The product obtained is a vermiculite-aluminum oxide nanocomposite.

2.2.2 Characterization of prepared nnocomposites

For the characterization of nanocomposites, SEM, XRD, FTIR, and BET analyses were performed using Hitachi S3240 SEM equipment (Japan), Bruker Tensor27 FTIR equipment (USA), Quantachrome NOVA2000 XRD equipment, and TMAX-3H-2000PS1 BET surface area analyzer, respectively.

2.2.3 Batch experiments

To conduct this research, a certain amount of potassium nitrate in DI water was used to prepare the desired concentrations of nitrate ions. After designing the solution, adsorption in the batch system was studied, and the effects of factors affecting the studied process were investigated. These factors included contact time, pH, concentration of salt, and adsorbent dosage. To perform adsorption experiments, the adsorbent and the synthetic solution were first placed in an Erlenmeyer and stirred at 200 rpm. After a specific time, centrifugation separates the adsorbent from the solution. The adsorption amount was determined using atomic absorption spectrophotometry at 275 nm. The removal percentage was obtained according to the following equation [12]:

$$R(\%) = \frac{C_i - C_e}{C_i} \times 100 \tag{1}$$

C_i and C_e are the initial concentration of nitrate ions and the final concentration (mg/L), respectively. Additionally, the adsorption capacity can be obtained using equation 2 [13]:

$$q_{eq} = \frac{C_o - C_e}{m} \times V \tag{2}$$

where C_e (mg/L), C_o (mg/L), V (L), and m (g) are the equilibrium concentration of nitrate ion, the initial concentration of nitrate ion volume of the solution, and the mass of the adsorbent, respectively.

2.2.4 Investigation of adsorption kinetics

The kinetic models, including pseudo-first-order, pseudo-second-order, and intra-particle diffusion (IPD) models, were used to demonstrate the adsorption mechanism. These models are expressed by equations 3, 4 and 5, respectively [14]:

$$\ln(q_e - q_t) = \ln(q_e) - K_1 \tag{3}$$

$$\frac{t}{q_t} = \frac{1}{K_2 - q_e^2} + \frac{t}{q_e} \tag{4}$$

$$q_t = K_{id} t^{1/2} + C \tag{5}$$

where q_e and q_t are the equilibrium and adsorption capacity at time t (min), respectively, K_1 is the first-order rate constant (min^{-1}), K_2 is the second-order rate regular (g/mg·min), and K_{id} is the intra-particle diffusion rate constant (mg/g·min$^{0.5}$).

2.2.5 Adsorption isotherm investigation

The adsorption isotherm models were used to evaluate the adsorption rate under different conditions. The following

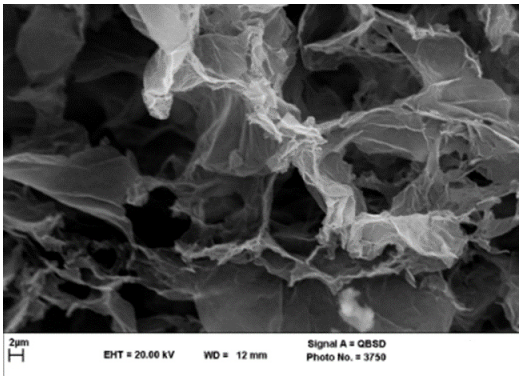

Figure 1. Vermiculite structure SEM image.

equations express these models. The Langmuir equation is expressed by equation 6:

$$(\frac{x}{m}) = q_e = q_{max}(\frac{b \times C_e}{1 + K_l \times C_e}) \quad (6)$$

K_L is the Langmuir adsorption equilibrium constant, q_{max} is the maximum adsorption capacity, and C_e (mol/L) is the equilibrium concentration of the adsorbed substance.
The Freundlich equation is given by equation 7 [15]:

$$q_e = (\frac{x}{m}) = K_f \times C_e^{1/n} \quad (7)$$

Here, K_F (mg/g) $(mg/L)^{(-1/n)}$ is the Freundlich adsorption capacity constant.
The Temkin isotherm equation is as follows [16]:

$$q_e = \frac{RT}{b_T} \ln(A_T C_e) \quad (8)$$

$$q_e = \frac{RT}{b_T} \ln(A_T) + \frac{RT}{b_T} \ln(C_e) \quad (9)$$

In the above equations, A_T (L/g) is the Temkin equilibrium constant related to the maximum binding energy, and b_T (J/mol) is the Temkin equilibrium constant related to heat of adsorption.
The Redlich-Peterson model combines variables into a single empirical equation [17]:

$$q_e = \frac{K_{RP} C_e}{1 + \alpha_{RP} C_e^{\beta}} \quad (10)$$

In linearized form, it becomes:

$$\frac{C_e}{q_e} = \frac{\alpha_{RP} C_e^{\beta}}{K_{RP}} + \frac{1}{K_{RP}} \quad (11)$$

K_{RP}, α_{RP}, and β are the Redlich-Peterson parameters in the above equations. The logarithmic form of the equation is as follows:

$$\ln(\frac{C_e}{q_e}) = \ln(\frac{\alpha_{RP}}{K_{RP}^2}) + \beta \ln(C_e) \quad (12)$$

2.2.6 Thermodynamics analysis

At the temperatures of 25, 35, and 45 °C, thermodynamic factors, including enthalpy in kJ/mol, entropy in kJ/(mol.K), and Gibbs free energy, are as follows [18]

$$K_d = \frac{q_e}{C_e} \quad (13)$$

where K_D is the adsorption equilibrium constant (L/mg).
The change in Gibbs free energy is as follows [19]

$$\Delta G^0 = -RT \ln(K_D) \quad (14)$$

The change in entropy is determined using the following equation:

$$\Delta G^0 = \Delta H^0 - T\Delta S^0 \quad (15)$$

$$\ln(K_D) = \frac{\Delta S^0}{R} - \frac{\Delta H^0}{R} \frac{1}{T} \quad (16)$$

If ΔG^0 is hostile, it indicates the spontaneity of the process. If ΔG^0 is positive, it suggests non-spontaneity of the

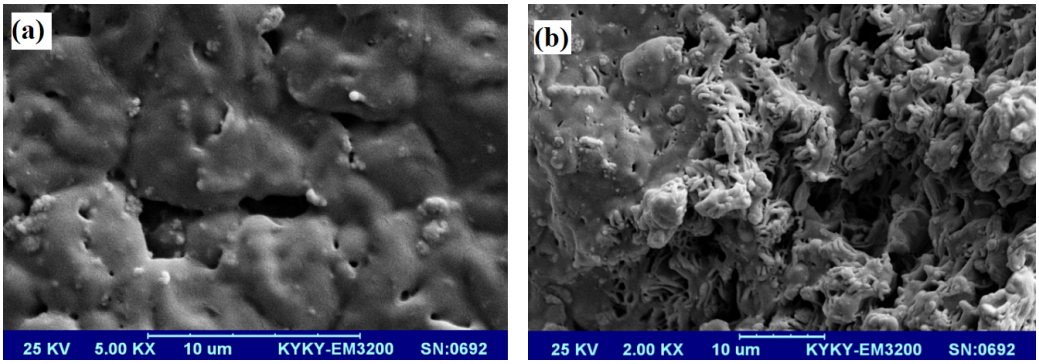

Figure 2. SEM Images (a) Vermiculite/Aluminum Oxide (Before Adsorption), (b) Surface of Vermiculite/Aluminum Oxide Adsorbent (After Adsorption).

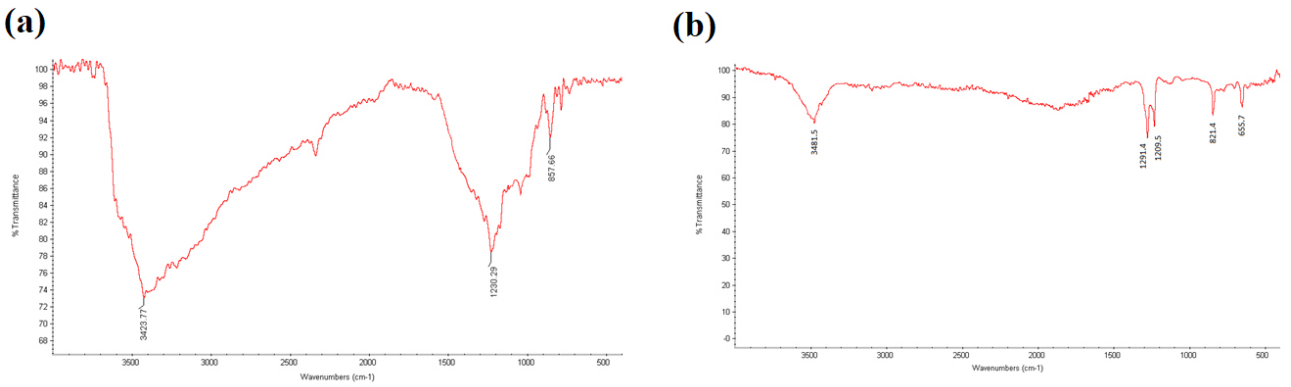

Figure 3. FTIR spectra of prepared samples, a) vermiculit and b) vermiculite/aluminum oxide samples.

process, and if ΔG^0 is equal to 0, it means the process is at equilibrium. If ΔH^0 is negative, it indicates exothermic adsorption; if ΔH^0 is positive, it suggests endothermic adsorption.

3. Results

3.1 Characterization of nanocomposites

The SEM results of samples scanning electron microscopy (SEM) for vermiculite and vermiculite/aluminum oxide before and after adsorption are shown in Figures 1 and 2, respectively. The vermiculite structure appears as a layered structure with dimensions smaller than 100 nanometers in Figure 1. In Figure 2(a), aluminum oxide nanoparticles can be observed within the vermiculite structure. In Figure 2(b), after adsorption, it can be seen that pollutant particles have occupied the porous and empty regions of the adsorbent.

FTIR analysis for the synthesized samples is presented in Figure 3 . For vermiculite, peaks at 3423 cm^{-1}, 1230 cm^{-1} and 857 cm^{-1} are related to the hydroxyl group, the Si-O bond, and the Al-O bound, respectively.

In the case of the vermiculite/aluminum oxide nanocomposite, peaks related to vermiculite are observable. Additionally, peaks at 655 cm^{-1} are indicative of Al-O bond vibrations. So, it is clear that the nanocomposite synthesis is successful.

The results of the BET analysis are given in Figure 4 and Table 1. As observed, vermiculite exhibits an isotherm of type IV, indicating the presence of both micropore and mesopore structures [12].

The surface area for vermiculite and vermiculite/aluminum oxide nanocomposite is 326.3 and 663.6 m^2/gr, respectively. As can be seen, aluminum oxide incorporation into vermiculite causes an increase in specific surface area, resulting in improved adsorption efficiency.

3.2 The parameter's effect on adsorption

3.2.1 pH

The ionization of the adsorbent functional groups and the control of the interaction between the pollutant and the adsorbent are influenced by the pH of the aqueous medium. The pH values for vermiculite and vermiculite/aluminum oxide were 2.8 and 3.5, respectively. Aluminum oxide reduces the negative surface charge of vermiculite. Accordingly, the effect of pH on the removal of nitrate ions is shown in Figure 5, with increasing pH from 2 to 5. The adsorption efficiency of nitrate ions by vermiculite/aluminum oxide changes from 42.2% to 99.3%. pH lower than 5 increases the concentration of hydronium ions in the medium. Ions react with aluminum oxide on the adsorbent surface and lead to the formation of $AlOH^+$. As a result, the surface charge becomes a positive [15]. Therefore, at pH values lower than 5, the positively charged adsorbent absorbs the negatively charged nitrate ions. At pH values higher than 5, the concentration of hydroxide

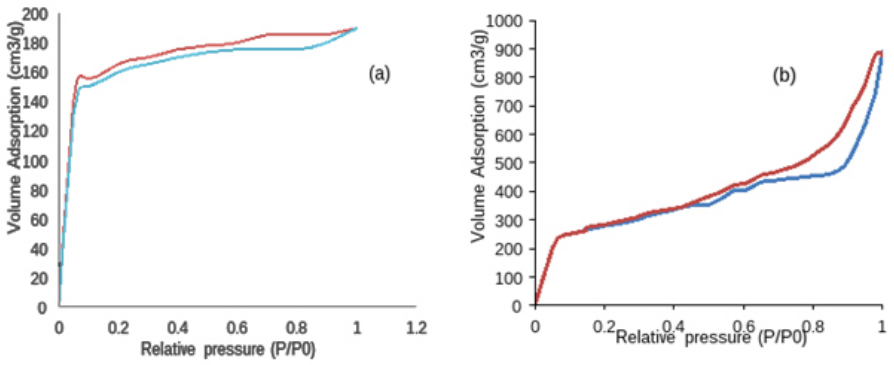

Figure 4. BET analysis for (a) vermiculite and (b) vermiculite/aluminum oxide.

Table 1. Structural parameters obtained from BET analysis.

	Total surface area (m^2g^{-1})	Total pore volume (cm^3g^{-1})	Mean pore size (nm)
Vermiculite	326.3	0.05	2.3
Vermiculite/aluminum oxide	663.6	0.56	4.9

ions increases, and the positive surface charge decreases, leading to electrostatic repulsion between nitrate ions and the surface, reducing adsorption efficiency.

3.2.2 Contact time

The effect of contact time on the nitrate removal percentage is shown in Figure 6. As observed, the nitrate removal rate increases with increasing contact time for the nanocomposite adsorbent. Additionally, the removal rate is rapid in the first 50 minutes. Therefore, this time (maximum value) is considered in subsequent tests. This increase over time is related to unsaturated and accessible sites for nitrate adsorption. With time, these sites become saturated, so after 50 minutes, the active sites are almost saturated, and the removal rate remains constant.

3.2.3 Adsorbent dosage

As observed in Figure 7, by increasing the adsorbent dosage from 0.5 to 1.5 gr/L, the percentage of nitrate elimination gradually increases from 33.2% to 99%. The reason for this increase is the more significant number of available adsorption sites. Therefore, the subsequent sections considered 1.5 grams per liter of the adsorbent suitable for acceptable nitrate removal.

3.2.4 Checking the initial size of nitrate in solution

Figure 8 shows the initial concentration of Nitrate on the removal efficiency by nanocomposite adsorbents. The vermiculite/aluminum oxide nanoabsorbent increases with nitrate removal and increases the initial concentration from 20 mg/L to 50 mg/L due to the improved driving force to overcome. All the resistances related to the mass transfer between the liquid phase and the adsorbent when the value is higher than 50 mg/L, nitrate removal is reduced despite the increase in driving force. The desired reduction is due to the saturation of the absorption sites in the adsorbents. Above, the adsorbents' absorption sites reach the saturation limit, reducing the absorption efficiency [14].

3.2.5 Temperature

The effect of temperature on the nitrate removal percentage is illustrated in Figure 9. As can be seen, increasing temperature has an increasing impact on the adsorption capacity. Therefore, it can be inferred that this adsorption reaction is endothermic. The adsorption capacity increases since an increase in temperature leads to greater molecular mobility and more effective collisions between nitrate ions and the adsorbent. Additionally, an increase in temperature causes the expansion and enlargement of the pore volume, leading to a rise in the number of active sites on the adsorbent's surface and within the pore structures.

4. Investigation of adsorption isotherms

The adsorption isotherm evaluation is presented in Figure 10 and Table 2. By comparing the graphs and linear regression of the curves, it can be concluded that the experimental data is consistent with the Langmuir model, indicating that nitrate adsorption on the synthesized adsorbent occurs as a monolayer.

To express the main characteristic of the adsorption isotherm, the separation factor (RL) in the Langmuir model, which is a dimensionless constant, is used and serves to evaluate adsorption. This factor is defined as follows

$$R_L = \frac{1}{1 + bC_{max}} \tag{17}$$

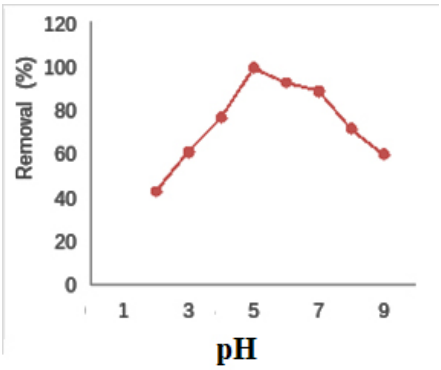

Figure 5. Effect of pH on the percentage of nitrate removal from aqueous solution by the synthesized nanocomposites.

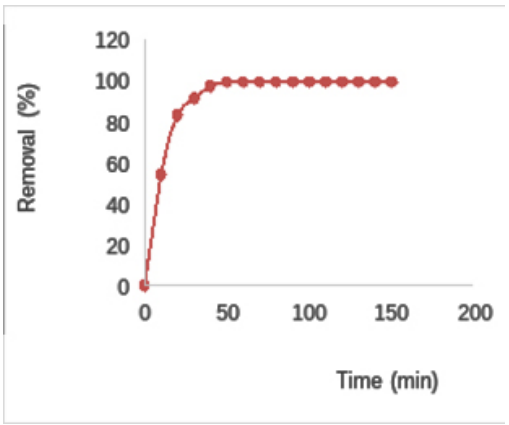

Figure 6. Effect of contact time on nitrate removal.

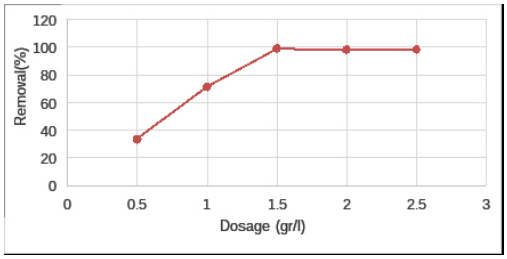

Figure 7. Effect of Adsorbent Dosage on the nitrate removal (Contact Time: 50 minutes, Optimal Adsorbent Dosage: 1.5 gr/l, pH: 5, Initial Nitrate Concentration: 50 mg/L).

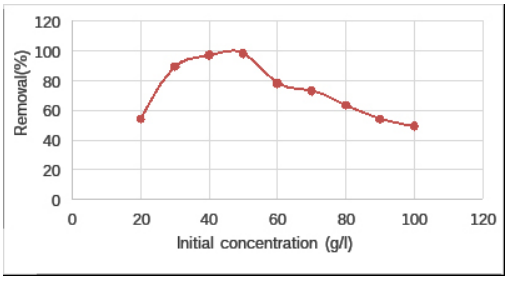

Figure 8. Effect of the initial concentration of nitrate solution on the removal percentage by the synthesized nanocomposite adsorbent.

where C_{max} is the initial concentration of the nitrate ions in the solution when the value of the separation factor is between zero and one, the adsorption process is considered favorable. When it is greater than 1, it is considered unfavorable. Therefore, considering the concentration of Nitrate in the range of 10 to 100 milligrams per liter, the values of the separation factor for the vermiculite/aluminum oxide nanocomposite fall in the range of 0.083 to 47.0, indicating the desirability of the adsorption process.

4.1 Investigation of adsorption kinetic

The results of the kinetic models for nitrate adsorption by the synthetic adsorbent are shown in Figure 11.
From the comparison of the figures, it can be inferred that the nitrate ion adsorption process by the adsorbent conforms to a pseudo-second-order kinetic model. The rate constant of the pseudo-second-order kinetic model at concentrations ranging from 20 to 90 milligrams per liter has been determined using the obtained linear equations and is reported in Table 3.

In Figure 11, an intra-particle diffusion model for the adsorbent has been investigated. Based on the figure, a phase (line) in the diffusion plot indicates that intra-particle diffusion alone does not control adsorption. Instead, the surface adsorption process is initiated by diffusing pollutant particles to the adsorbent surface in the first phase and then continues through intra-particle diffusion in the subsequent phase. Therefore, the surface adsorption mechanisms are uniform at different contact times, and both phases play an equal role in limiting the rate of surface adsorption [15–17].

Table 2. Parameters obtained from the adsorption models of nitrate ions by vermiculite/aluminum oxide nanocomposite adsorbent.

Adsorption isotherm model		
Langmuir	C_{max}(mg/g)	90.9
	K_L(L/mg)	0.11
	R^2	0.99
Freundlich	K_F(L/g)	22.6
	N	3.2
	R^2	0.93
Temkin	A_T(L/g)	11.82
	b_T(j/mol)	138.6
	R^2	0.97
Redlich-Peterson	K_{RP}(L/g)	58.8
	a_{RP}(L/mg)	1.35
	β	0.67
	R^2	0.96

4.2 Investigation of adsorption thermodynamics

Since the adsorption process for nitrate ions by the studied adsorbents conforms better to the Langmuir isotherm, the parameter "b" from this isotherm can be used to investigate the thermodynamics of the adsorption process.

$$(\frac{x}{m}) = q_e = q_{max}\frac{b \times C_e}{1 + b \times C_e} \tag{18}$$

The temperature-dependent relationship for the coefficient b in the Langmuir isotherm is used to calculate the isosteric heat of the surface adsorption process. This temperature relationship is defined as $b \approx \exp(-\Delta H/RT)$ and is incorporated into the Langmuir equation.

$$q_e = q_{max}\frac{bT \times C_e}{1 + b(T) \times C_e} \tag{19}$$

The b coefficient expresses the adsorption strength adsorption. The temperature dependence of this coefficient is in the form of equation 20:

$$b(T) = b_\infty \frac{-\Delta H}{RT} \tag{20}$$

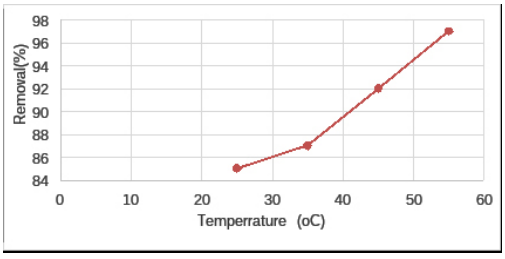

Figure 9. Effect of temperature on nitrate removal percentage by adsorbent.

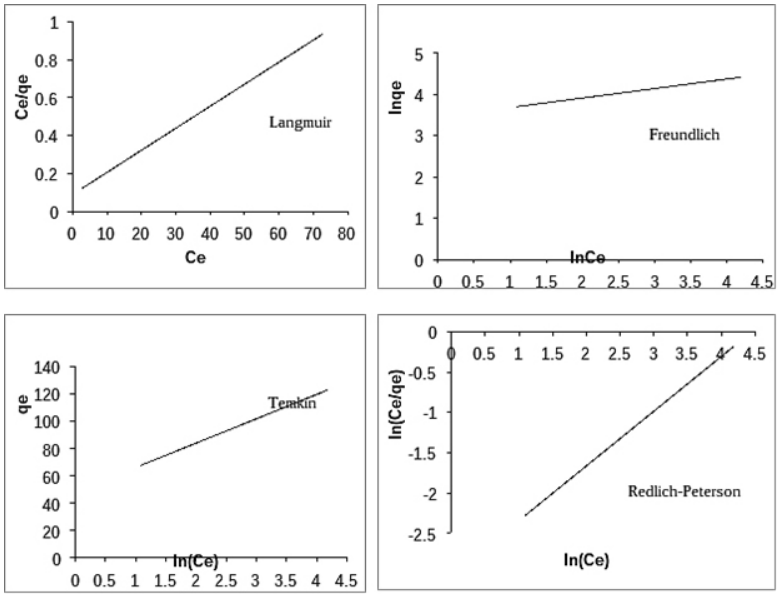

Figure 10. Investigation of linear models for the adsorption isotherm of nitrate ions by vermiculite/aluminum oxide nanocomposite adsorbent.

Its linear form is as follows:

$$\ln(b) = -\frac{\Delta H}{R}\frac{1}{T}\ln(b_\infty) \tag{21}$$

The parameter b_∞ shows the tendency to absorb at high temperatures. If we have the changes of b with temperature, the process is calculated from $\ln(b)$ in terms of $1/T\Delta H$ (Table 4).

The figure shows that the absorption process is endothermic, and the absorption increases with increasing temperature because the absorption process is guided by both absorption and activation energy. The absorbed heat equals the surface absorption enthalpy of the physically absorbed species [20]. The change in Gibbs free energy (ΔG) is expressed by equa-

Table 3. Kinetic constants obtained from the nitrate ion adsorption process by ermiculite/aluminum oxide adsorbent.

C_0 (mg/l)	q_e	K_2	R^2
20	0.85	0.06	0.98
30	0.91	0.049	0.97
50	0.91	0.031	0.99
70	1.13	0.019	0.98
90	1.67	0.01	0.98

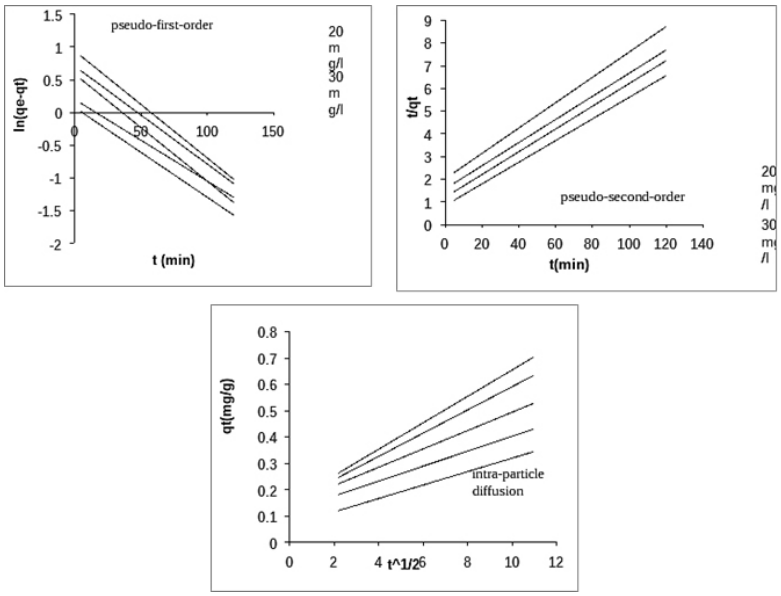

Figure 11. Investigating kinetic models of nitrate ion adsorption by vermiculite/aluminum oxide nanocomposite adsorbent.

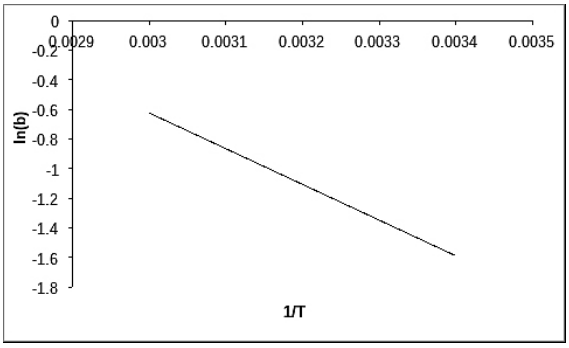

Figure 12. Linear drawing of parameter b regarding the inverse of temperature in nitrate ion adsorption process by vermiculite/aluminum oxide adsorbent.

tion 22:

$$\Delta G = -RT\ln(K_c) \tag{22}$$

In the above equation, K_C is the equilibrium constant and is calculated according to the following equation:

$$K_c = \frac{C_{adsorp}}{C_{equlibrium}} = \frac{C_0 - C_e}{C_e} \tag{23}$$

The following equation is used to calculate entropy changes:

$$\ln(K_c) = \frac{\Delta S^0}{R} - \frac{\Delta H^0}{RT} \tag{24}$$

The results are presented in Table 5.

5. conclusion

The most important findings from the present study can be summarized as follows:

• We are increasing the contact time to 50 minutes, increasing the adsorption percentage.

• Increasing the adsorbent dose up to 1.5 grams per liter increases the percentage of adsorption, after which it becomes constant.

• We are increasing the initial nitrate concentration to 50 mg/, a percentage of adsorption. By further growing, this value decreases.

• With an increase in the initial nitrate concentration up to 50 milligrams per liter, the removal efficiency increased for the Nano-adsorbent vermiculite/aluminum oxide, but then.

• An increase in pH from 2 to 5 led to an increase in removal efficiency, but further increases in pH reduced the removal efficiency.

• The adsorption capacity of the adsorbent increases with temperature increasing.

• The Langmuir isotherm model provides a consistent insistent for the adsorbent's nitrate consistency.

• The second-order kinetic model was more suitable for predicting the adsorption process rate.

• The negative sign of the Gibbs free energy indicates the spontaneity and the tendency of nitrate ions to be adsorbed by the adsorbent.

• The positive enthalpy illustrates the endothermic nature of the adsorption process.

The positive sign of the change in entropy suggests an increase in entropy within the system, increased particle dispersion at the liquid-solid interface, and increased adsorbed par, and the adsorbent energy findings provide valuable insights into the adsorption of nitrate ions using the synthesized adsorbent and its potential for water treatment applications.

Table 4. Changes of Langmuir isotherm constants with temperature in the nitrate ion absorption process by the adsorbent.

T (°C)	T (K)	$1/T$ (1/K)	b (l/mg)	Ln(b)
25	298	0.0033	0.11	-2.2
35	308	0.0032	0.22	-1.5
45	318	0.0031	0.35	-1.04

Table 5. Equilibrium constant, Gibbs free energy, and entropy at different temperatures.

T (K)	C_e (mg/l)	K_c	ΔG^0 (j/mol)	ΔS^0 (j/molK)
298	7.7	5.49	-4219.12	103.03
308	6.8	6.35	-4748.16	93.21
318	5.9	8.76	-5737.67	89.91

Ethical approval:
This manuscript does not report on or involve the use of any animal or human data or tissue. So the ethical approval does not applicable.

Funding:
All the experimental stages of this paper have been done in the laboratories of Azad University and do not include the cost from external sources.

Authors Contributions:
All authors have contributed equally to prepare the paper.

Availability of data and materials:
The data that support the findings of this study are available from the corresponding author upon reasonable request.

Conflict of Interests:
The authors declare that they have no known competing financial interests or personal relationships that could have appeared to influence the work reported in this paper.

References

[1] S.E.S. Ghazy, A.A.H. El-Asmy, and A.M. EL-Nokrashy. "Separation of chromium(III) and chromium(VI) from environmental water samples.". *International Journal of Industrial Chemistry*, **2**:242–252, 2011.

[2] A.A. Beni and A. Esmaeili. "Biosorption, an efficient method for removing heavy metals from industrial effluents: A Review.". *Environmental Technology & Innovation*, **17**:100503, 2020.

[3] N. Leopold and B. Lendl. "A new method for fast preparation of highly surface-enhanced Raman scattering (SERS) active silver colloids at room temperature by reduction of silver nitrate with hydroxylamine hydrochloride.". *Journal of Physical Chemistry B*, **107**: 5723–5727, 2003.

[4] A. Esmaeili and A.A. Beni. "Novel membrane reactor design for heavy-metal removal by alginate nanoparticles.". *Journal of Industrial and Engineering Chemistry*, **26**:122–128, 2015.

[5] J. Aravind, S. Muthusamy, S.H. Sunderraj, L. Chandran, and K. Palanisamy. "Pigeon pea (Cajanus cajan) pod as a novel eco-friendly biosorbent: a study on equilibrium and kinetics of Ni (II) biosorption.". *International Journal of Industrial Chemistry*, **4**:1–9, 2013.

[6] O.M. Abdallaha and A.M. Badaweyb. "Determination of amlodipine and valsartan in binary mixture using derivative- ratio spectrophotometric, chemometric and high performance liquid chromatographic-UV methods.". *International Journal of Industrial Chemistry*, **2**:131–139, 2011.

[7] L.T. Popoola, A.S. Grema, G.K. Latinwo, B. Gutti, and A.S. Balogun. "Corrosion problems during oil and gas production and its mitigation.". *International Journal of Industrial Chemistry*, **4**:1–15, 2013.

[8] S. Kango, S. Kalia, A. Celli, J. Njuguna, Y. Habibi, and R. Kumar. "Surface modification of inorganic nanoparticles for development of organic–iorganic–inorganicosites—A review.". *Progress in Polymer Science*, **38**:1232–1261, 2013.

[9] A. Esmaeili and A.A. Beni. "A novel fixed-bed reactor design incorporating an electrospun PVA/chitosan nanofiber membrane.". *Journal of hazardous materials*, **280**:788–796, 2014.

[10] A. Esmaeili and E. Sadeghi. "The efficiency of penicillium commune for bioremoval of industrial oil.". *International Journal of Environmental Science and Technology*, **11**:1271–1276, 2014.

[11] A.M. Awwad, N.M. Salem, and A.O. Abdeen. "Green synthesis of silver nanoparticles using carob leaf extract and its antibacterial activity.". *International journal of Industrial chemistry, 4 (2013) 1-6*, **4**:1–6, 2013.

[12] S. Samatya, N. Kabay, Ü. Yüksel, M. Arda, and M. Yüksel. "Removal of Nitrate from aqueous solution by nitrate selective ion exchange resins.". *Reactive and Functional Polymers*, **66**:1206–1214, 2006.

[13] N. Öztürk and T.E.l. Bektaş. "Nitrate removal from aqueous solution by adsorption onto various materials.". *Journal of Hazardous Materials*, **112**:155–162, 2004.

[14] D.S. Powlson, T.M. Addiscott, N. Benjamin, K.G. Cassman, T.M. De Kok, H. Van Grinsven, J.L. L'Hirondel, A.A. Avery, and C. Van Kessel. "When does Nitrate become a risk for humans.". *Journal of Environmental Quality*, **37**:291–295, 2008.

[15] M. Shrimali and K. Singh. "New methods of nitrate removal from water.". *Environmental Pollution*, **112**: 351–359, 2001.

[16] A. Kapoor and T. Viraraghavan. "Nitrate removal from drinking water.". *Journal of Environmental Engineering, 123 (1997) 371-380*, **123**:371–380, 1997.

[17] S.K. Sharma and R.C. Sobti. "Nitrate removal from ground water: a review.". *E-Journal of Chemistry*, **9**: 1667–1675, 2012.

[18] S.S. Sologubov, A.V. Markin, Y.A. Sarmini, N.N. Smirnova, K.L. Boldyrev, E.A. Tatarinova, I.B. Meshkov, and A.M. Muzafarov. "Thermodynamic investigation of G2 and G4 siloxane dendrimers with trimethylsilyl terminal groups.". *The Journal of Chemical Thermodynamics*, **153**:106318, 2021.

[19] N.M. Mahmoodi, B. Hayati, M. Arami, and C. Lan. "Adsorption of textile dyes on pine cone from colored wastewater: kinetic, equilibrium and thermodynamic studies.". *Desalination*, **268**:117–125, 2011.

[20] N.M. Crawford. "Nitrate: nutrient and signal for plant growth.". *The Plant Cell*, **7**:859–868, 1995.